Dental Materials 39 (2023) 648–658

Contents lists available at ScienceDirect

Dental Materials

journal homepage: www.elsevier.com/locate/dental

Effect of airborne particle abrasion treatment of two types of 3D-printing resin materials for permanent restoration materials on flexural strength☆

You-Jung Kang[a,1], Hoon Kim[b,c,1], Jiho Lee[c], Yeseul Park[a], Jee-Hwan Kim[a,*]

[a] Department of Prosthodontics, Oral Science Research Center, College of Dentistry, Yonsei University, Seoul, the Republic of Korea
[b] Research Institute of Agriculture and Life Sciences, College of Agriculture & Life Sciences, Seoul National University, Seoul 08826, the Republic of Korea
[c] Graphy, Inc. 6th Fl, Ace GasanFORHU, 225 Gasan digital 1-ro, Geumcheon-gu, Seoul 08501, the Republic of Korea

ARTICLE INFO

Keywords:
3D-printing resin
Flexural strength
Surface treatment
Airborne-particle abrasion
Weibull analysis
Dynamic mechanical analysis
Nano-indentation

ABSTRACT

Objectives: This study aimed to assess the effects of airborne-particle abrasion (APA) on the flexural strength of two types of 3D-printing resins for permanent restoration.
Methods: Two types of 3D printing resins (urethane dimethacrylate oligomer; UDMA, ethoxylated bisphenol-A dimethacrylate; BEMA) constituting different components were printed. The specimen surfaces were subjected to APA using 50 and 110 μm alumina particles under different pressures. The three-point flexural strength was measured for each surface treatment group, and a Weibull analysis was performed. Surface characteristics were analyzed *via* surface roughness measurements and scanning electron microscopy. Dynamic mechanical analysis and nano-indentation measurements were limited to the control group.
Results: The three-point flexural strength according to the surface treatment was significantly lower in the UDMA group for large particle sizes and at high pressures; the BEMA group demonstrated low flexural strength for large particle sizes regardless of the pressure. After thermocycling, the flexural strengths of UDMA and BEMA significantly decreased in the group subjected to surface treatment. The Weibull modulus and characteristic strength of UDMA were higher than those of BEMA under different APA and thermocycling conditions. As the abrasion pressure and particle size increased, a porous surface formed, and the surface roughness increased. Compared with BEMA, UDMA featured a lower strain, greater strain recovery, and a negligible increase in modulus according to strain.
Significance: Thus, surface roughness increased with the sandblasting particle size and pressure of the 3D-printing resin. Hence, a suitable surface treatment method to improve adhesion can be determined by considering physical property changes.

1. Introduction

Advances in the computer-aided design and manufacturing (CAD/CAM) technology have facilitated the production of inlays, crowns, and dentures using 3D printers and polymers. These developments have yielded distinct benefits for the dental community. Consequently, the digitalization of dental care has reduced working times and labor compared with conventional methods, facilitating easy and accurate reproductions of small and delicate teeth; moreover, the approach is economically competitive [1–4]. Notably, the 3D-printing resin materials currently used for temporary restorations in clinical practice feature excellent mechanical properties and color stability, lower polymerization shrinkage compared with self-curing resins for existing temporary restorations, and better margin suitability than CAD/CAM milling-based materials. Moreover, the mechanical performance of these materials under various conditions, such as output and surface treatment, has been extensively studied [5–11]. Recently, resins for 3D printing that can be used as final prostheses are continuously being developed. These 3D-printing resins for permanent restorations comprise urethane dimethacrylate (UDMA), esterification products of 4, 4′-isopropylidenediphenol, ethoxylated, and 2-methylprop-2-enoic acid, and ethoxylated bisphenol-A dimethacrylate (Bis-EMA). Notably, using

☆ Supported by the Korea Medical Device Development Fund (KMDF) grant funded by the Korea government (MSIT) (Grant nos. KD0002603G0003011 or RS-2020-KD000260).

* Correspondence to: Department of Prosthodontics, Yonsei University College of Dentistry, 50-1 Yonsei-ro, Seodaemun-gu, Seoul 03722, the Republic of Korea.
E-mail address: jee917@yuhs.ac (J.-H. Kim).

[1] These authors contributed equally to this work as first authors.

https://doi.org/10.1016/j.dental.2023.05.007
Received 7 November 2022; Received in revised form 2 May 2023; Accepted 8 May 2023

the same acrylic photolithography system can lead to considerable changes in the physical properties of products, depending on the resin type and its composition, particularly its constituting monomers and oligomers. Each 3D printing resin manufacturer uses different types of raw materials and composites. Consequently, the structures and monomer selections of urethane acrylate oligomers affect the mechanical properties of the final 3D-printed prosthetics [12–16].

Generally, dental restorations require prosthetic materials with appropriate mechanical properties, accuracy, color stability, and hardness to function over the long term [17–19]. This is because when the final prosthesis is exposed to a wet environment and functional stress in the oral cavity over an extended period, the strength and stability of the material may decrease owing to deterioration, leading to a risk of adhesion failure [17,20]. Therefore, evaluating the mechanical properties of 3D-printing resins used for the final prosthesis is essential.

The primary clinical challenge in using 3D printing resins for long-term definitive restorations is ensuring appropriate bonding between the resins and cement or teeth. While extensive research is underway to improve the binding force, airborne-particle abrasion (APA) is commonly employed in dental prostheses, including zirconia, metal, and polymeric CAD/CAM blocks, to enhance the bonding strength [21,22]. In particular, APA can improve adhesion by removing surface impurities and increasing roughness, energy, and hydrophilicity. Moreover, grinding and sandblasting CAD-CAM temporary restorative resins can improve their bonding with existing temporary restorative resins for repair [21,23]. High-performance polymers are inert surfaces; therefore, pretreatment is essential for successful bonding. Previous studies have demonstrated that polyaryletherketone (PAEK)-based polyetheretherketone (PEEK) materials can increase their adhesion with methylmethacrylate (MMA)-based adhesives when treated with APA [24]. Additionally, sandblasting, as a method of repairing or relining a 3D printable polymer for a temporary prosthesis with an existing repair polymer, is capable of increasing the bonding strength with the relining material [23]. Therefore, optimizing the conditions for APA, such that the mechanical properties of the resin are retained while the adhesion between the resin cement and permanent resin is enhanced, is necessary.

There are several methods for evaluating the mechanical properties of a material. Among these, the dynamic mechanical analysis (DMA) can be used to analyze the rheological behavior of materials. Based on this method, one can compare the behavior of a material exposed to rapid and slow deformation using the frequency sweep mode. At high frequencies, the surface behavior of the material during sandblasting can be predicted by observing the resin used for the crown, whereas at low frequencies, creep deformation of the material can be predicted [25]. Further, nano-indentation can be used to analyze the surface behavior of prostheses resulting from external forces. This approach is effective in analyzing the microscopic behavior of the material surface because it analyzes the behavior at the sub-micro level [26–28].

However, reports on the surface treatment of 3D printing resins for final prostheses are virtually non-existent. Nevertheless, assessing the changes in physical properties according to the composition and surface treatment of the permanent resin and identifying optimal APA conditions are crucial [25]. Accordingly, this study aims to investigate the effect of varying APA conditions on the flexural strengths of two types of 3D-printing resins used as final prostheses. The hypothesis of this *in vitro* study hypothesizes that the APA surface treatment does not affect 3D-printing material properties.

2. Materials and methods

A flowchart describing the experimental procedure is presented in Fig. 1.

2.1. Materials

Two types of permanent restorative materials, that is, UDMA (Tera Harz TC-80DP A2, Graphy, Seoul, Korea) and Bis-EMA (BEMA), (Permanent Crown A2, Formlabs, Somerville, MA, USA) were used in this study for 3D printing. Moreover, alumina particles with sizes of 50 and 110 μm were used for the APA treatment (Table 1).

2.2. Sample preparation

All specimens were designed using a 3D modeling software (Meshmixer 3.1.373; Autodesk, San Rafael, CA, USA). For the flexural strength test, the specimens were designed to have a length of 25 mm and width and thickness of 2 mm, according to the ISO10477 standard. The specimens for nano-indentation, morphological, and roughness analyses were designed to have a diameter of 20 mm and a thickness of 2 mm. For the DMA, specimens were designed to have a length of 60 mm, width of 12.5 mm, and thickness of 3.3 mm. A standard tessellation language file was exported and used to manufacture all specimens using the two types of permanent dental materials. Each specimen was printed according to the manufacturer's recommended conditions based on the method described below for the respective materials.

First, in the UDMA manufacturing process, specimens of poly-materials were printed using a digital light processing (DLP) 3D printer (Sprint Ray Pro 95, Sprint Ray Inc., LA, CA, USA) at constant room temperature (25 ℃) according to the resin mixing and printing

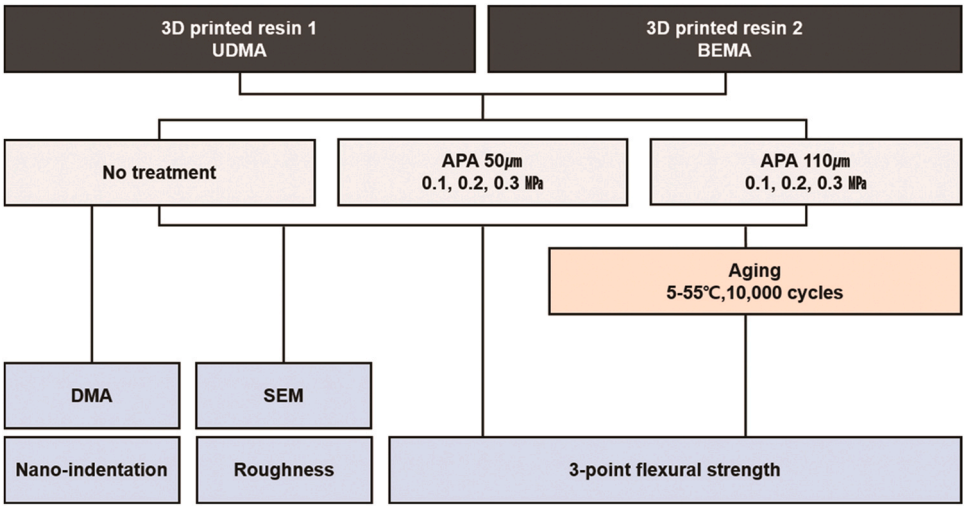

Fig. 1. Flowchart of the experimental procedure.

Table 1
Compositions of the materials used in this study.

Materials	Composition	Manufacturer
Tera Harz TC-80DP (A2)	Urethane dimethacrylate-based dental resin, phosphine oxides, pigment	Graphy, Seoul, Korea
Permanent Crown (A2)	Esterification products of 4,4′-isopropylidiphenol, ethoxylated and 2-methylprop-2enoic acid; ethoxylated bisphenol-A dimethacrylate (Bis-EMA, methacrylate polymer), silanized dental glass, methyl benzoylformate, diphenyl (2,4,6-trimethylbenzoyl) phosphine oxide (TPO, photoinitiator), 30–50 wt %—inorganic fillers (particle size 0.7 μm)	Formlabs, Somerville, MA, USA
Cobra Aluoxyd	50 μm aluminum oxide 100 μm aluminum oxide	Renfert GmbH, Hilzinger, Germany

The composition of the material is unknown as the company keeps it a trade secret.

parameters recommended by the manufacturer. To remove excess resins, the specimen was ultrasonically cleaned using 90 % isopropyl alcohol. After drying, it was cured for 20 min using a curing machine (Cure-M 102H, Graphy, Seoul, Korea) following the protocol recommended by the manufacturer.

The permanent resin printing process for the BEMA component was as follows: specimens of the materials were printed using a stereolithography (SLA) 3D printer (Form 3, Formlabs, Somerville, MA, USA) at constant room temperature according to the resin mixing and printing parameters recommended by the manufacturer. After washing and drying using the isopropyl alcohol solution, the specimen was cured for 30 min using a curing machine (Formcure, Formlabs, Somerville, MA, USA) according to the manufacturer's recommendations.

A total of 196 three-point flexural strength specimens were produced, and one specimen was reserved for each group for roughness and scanning electron microscopy (SEM) analyses. For the DMA and nano-indentation analyses, one specimen per material was printed. The resin specimens manufactured according to the conditions suggested by each manufacturer were randomly classified based on the abrasion conditions of the suspended particles.

UDMAC group: After printing with the UDMA resin, the samples were used without any treatment.

BEMAC group: After printing with the BEMA resin, the samples were used without any treatment.

UDMA *XY*: After printing with the UDMA resin, APA was performed using a sandblaster (Renfert Basic Classic; Renfert GmbH, Hilzingen, Germany) at a distance of 10 mm for 10 s with 50 and 110 μm aluminum oxide (Al_2O_3) particles (Cobra®, white; Renfert GmbH, Hilzingen, Germany) at pressures of 0.1, 0.2, and 0.3 MPa.

BEMA *XY*: After printing with the BEMA resin, APA was performed using a sandblaster at a distance of 10 mm for 10 s at particle sizes of 50 and 110 μm and pressures of 0.1, 0.2, and 0.3 MPa.

After the APA treatment, the treated specimens were washed in an ultrasonic cleaner for 5 min to remove alumina particles remaining on the surface. Note that the group name is indicated by the material abbreviation *XY* (*e.g.*, UDMA501), where X and Y indicate the particle size (μm) of Al_2O_3 and pressure (bar), respectively. In this study, a single operator was applied to the six sandblasting conditions.

The flexural strength specimens were separated before and after thermocycling. Half the specimens were stored in distilled water at 37 °C for 24 h. Moreover, half of the specimens in each group were subjected to 10,000 thermal cycles between 5 °C and 55 °C in distilled water (70 s per cycle; dwelling time: 30 s, transfer time: 5 s).

2.3. Three-point flexural strength

A three-point flexural strength test (n = 14) was performed using a jig in a universal testing machine (3366 Series, Instron Engineering, Norwood, MA, USA). The sample size was 25 × 2 × 2 mm (TWL). The distance between the specimen supports was 10 mm, and a loading force was applied to the specimens at a crosshead speed of 1 mm/min until the specimens fractured. The fracture load was recorded in Newtons, and the flexural strength (σ, MPa) was calculated according to the following relationship:

$$\sigma = \frac{3Fl}{2bh^2}$$

where F is the fracture load in Newtons, l is the span (distance between the centers of the supporting pins, 10 mm), b is the specimen width in millimeters, and h is the specimen height in millimeters.

2.4. Nano-indentation

Micro-indentation tests were performed to confirm the microscopic surface properties of the photocurable 3D printing resin intended for permanent restoration. For the specimen, control groups of the two types of 3D printing resins (UDMAC and BEMAC) were used (n = 1 for each resin group). A micro-indentation device (MCT^3 STeP4, Anton Paar GmbH, Graz, Austria) equipped with a Vickers diamond indenter was used in this test. The test conditions were as follows: 10 s loading time, 5 s pause time, and 10 s unloading time with indentation strengths of 2, 4, 6, 8, and 10 N. The samples had a diameter of 20 mm and thickness of 2 mm.

2.5. DMA

To quantify the mechanical dynamics and rheological properties of the photocurable 3D-printing resin for permanent restoration, a DMA (Q800, TA Instrument, New Castle, DE, USA) was performed at a mechanical dynamic analysis frequency between 0.01 and 100 Hz with a strain rate of 0.1 % based on the dual cantilever method. For the specimen, control groups of the two types of 3D printing resins (UDMAC and BEMAC) were used (n = 1 for each resin group). The sample size was 60 × 12.5 × 3.3 mm (TWL).

2.6. Surface characterization

To evaluate the differences according to APA conditions before thermocycling, the surface morphology of one representative specimen from each group was observed using a field emission scanning electron microscope (S-3000N, Hitachi, Tokyo, Japan). Further analyzes were performed after coating with platinum using an ion sputter coater (E-1010, Hitachi, Tokyo, Japan) at 500 and 2000 × magnification.

For topographic analysis and average surface roughness (R_a) determination of the 3D printed resin surfaces following different treatment methods before thermocycling, 14 specimens from each group were analyzed (n = one per group, nine points per specimen) using a 3D optical microscope (Contour GT-X3 BASE; Bruker Co., Bremen, Germany) in nine areas per sample. Subsequently, the average R_a value was calculated.

2.7. Statistical analysis

The final results were analyzed using a statistical software (SPSS 25.0, SPSS Inc., Chicago, IL, USA) by separately observing the resulting

flexural strength values of the groups. First, data normality was tested using the Kolmogorov–Smirnov test (with = 0.05). The flexural strength and roughness were analyzed based on a two-way analysis of variance (ANOVA) with the two types of materials. The surface treatment was regarded as an independent factor. For multiple comparisons, Bonferroni's multiple comparison test was used. The flexural strength according to artificial aging (before and after thermocycling) was analyzed using a t-test. ($\alpha = 0.05$).

Additionally, the flexural strength results obtained from the three-point bending test were analyzed using Weibull statistics to obtain the Weibull modulus (m) and characteristic stress (σ0) parameters. Accordingly, the failure and cumulative survival probabilities of the two 3D-printing resin materials under varying APA and thermocycling conditions were plotted for a comparative analysis. Additionally, the specific survival probabilities of the two materials at 50 MPa, 75 MPa, and 100 MPa were obtained calculated to compare their restoration performance in the clinic.

3. Results

3.1. Three-point flexural strength

The average flexural strengths and significant differences between UDMA and BEMA according to the surface treatment are presented in Fig. 2. The results of the two-way ANOVA, which was performed to verify the main effect and interaction effect of surface treatment conditions and materials on flexural strength, demonstrated that both surface treatment conditions ($F = 22.980$, $P < 0.001$) and materials ($F = 329.906$, $P < 0.001$) had a significant main effect. Furthermore, the interaction effect of surface treatment conditions and materials on flexural strength was also significant ($F = 8.805$, $P < 0.001$). In the post-hoc test, according to the surface treatment, the flexural strength decreased significantly with an increase in particle size and pressure. In addition, the UDMA group demonstrated a higher flexural strength than the BEMA group in the post- hoc test, according to the materials.

Before thermocycling, the average flexural strength of the UDMAC group was 143.6 ± 13.1 MPa, and no significant difference between the surface treatment groups, except UDMA1103, was observed. The UDMA1103 group presented a significantly lower flexural strength than the other surface treatment groups, averaging to a value of 122.9 ± 6.2 MPa. In the BEMAC group, the average flexural strength was 128.0 ± 22.4 MPa, and no significant difference between the 50 μm groups ($P < 0.001$) was observed; however, a significant difference between all 110 μm groups was noted. The flexural strength of the BEMA group was significantly lower than that of the UDMA group in both the control and surface treatment groups ($P < 0.05$). After thermocycling, the flexural strength of the UDMA group was significantly reduced over the entire surface treatment group compared to that of the control group, and no significant differences were observed within the surface treatment groups. In the BEMA group, no significant differences were observed between the groups.

When compared before and after thermocycling, in the UDMA group, the flexural strength presented a significant decrease for all the surface treatment groups, except for the UDMAC group. Moreover, in the BEMA group, the flexural strength presented a significant decrease for the BEMAC and the remainder of the surface treatment groups, except for the BEMA1102 and BEMA1103 groups. However, no significant difference was observed in the 0.2 and 0.3 MPa strengths of the 110 μm group. The UDMA group presented higher flexural strength than the BEMA group both before and after thermocycling.

Based on statistical data obtained from the Weibull analysis, the failure probabilities for all test groups were plotted as linear regressions (Supplementary Fig. S1). According to the graphs, thermocycling treatments appeared to decrease the probability curve. This corresponds to smaller values of characteristic strengths for the specimens after aging. In addition, the failure probability plots for both materials

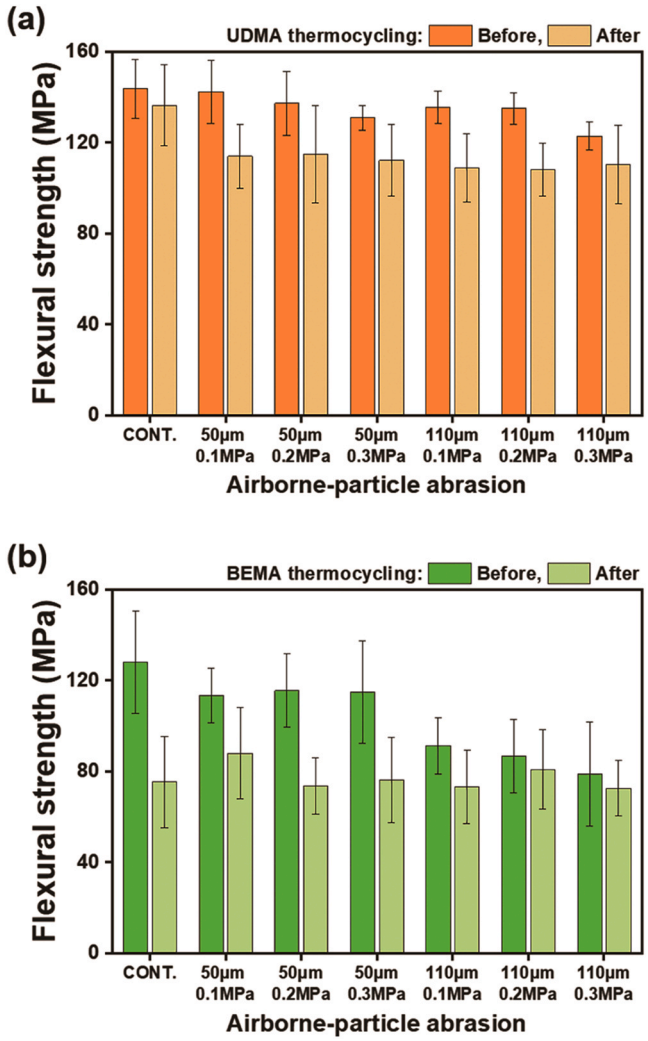

Fig. 2. Graph of the mechanical flexural strength and roughness behavior according to airborne-particle abrasion surface treatment. (a) UDMA and (b) BEMA flexural strength behavior according to the surface treatment conditions.

indicate more similar linear regression trends after thermocycling than those before thermocycling. Tables 2 and 3 summarize the flexural strength results obtained from the three-point bending test and the calculated Weibull parameters of the two 3D-printing materials under different APA and thermocycling conditions. The Weibull modulus (m), a measure of the strength distribution, represents the reliability of a material. The higher the Weibull modulus, the more consistent the material, and the narrower the probability curve. Generally, the characteristic strength (σ_o) can be employed to estimate the lifetime of a material. At the characteristic strength of a specimen, the probability of specimen failure is 63.2 %. Tables 2 and 3 present the R-squared values for each Weibull distribution regression. The results indicate that the UDMA groups exhibited a higher mean flexural strength, Weibull modulus, and characteristic strength than the BEMA groups under different APA and thermocycling conditions. After thermocycling, UDMA 502 presented the highest flexural strength. The Weibull survival probability plots, derived from the cumulative failure probability, are presented in Fig. 3. These plots comprehensively illustrate the failure of the product with increasing flexural strengths. The four plots indicate a general decrease in the survival rate with thermocycling treatment for both the 3D-printing resin materials and a greater survival rate for the UDMA group.

The specific survival probabilities at three flexural strength values of 50, 75, and 100 MPa are presented in Tables 4 and 5 to compare the two

Table 2
Weibull analysis of the biaxial flexural strengths for two different 3D printed resins before thermocycling with different APA conditions. (SD: standard deviation, *m*: Weibull modulus, σ_o: characteristic strength, N: number of samples, R^2: Weibull distribution regression).

APA (μm, bar)	Materials (before thermocycling)	n	Flexural strength (MPa)		Weibull statistics		
			Mean	SD	*m*	σ_o	R^2
C	UDMA	14	141.11[a]	9.1488	18.367	145.17	0.9552
	BEMA	14	125.68[a]	21.298	6.8275	134.48	0.9483
501	UDMA	14	141.35[a]	13.906	11.109	147.89	0.9082
	BEMA	14	111.99[a]	11.262	11.156	117.14	0.9321
502	UDMA	14	134.30[a,b]	8.1774	18.522	138.16	0.9123
	BEMA	14	112.88[a]	13.306	9.5685	118.80	0.9644
503	UDMA	14	130.02[a,b]	4.3020	35.767	131.99	0.9252
	BEMA	14	112.42[a]	21.042	5.4568	122.12	0.9018
1101	UDMA	14	134.52[a,b]	6.0902	25.946	137.31	0.9080
	BEMA	14	89.330[b]	10.348	9.8397	93.903	0.9642
1102	UDMA	14	133.82[a,b]	5.3355	29.502	136.28	0.9005
	BEMA	14	84.455[b]	14.160	6.8847	90.365	0.9179
1103	UDMA	14	121.77[b]	4.7078	30.860	123.90	0.9551
	BEMA	14	83.786[b]	6.7767	14.811	86.731	0.9730

C, control; UDMA, urethane dimethacrylate; BEMA, Bis-EMA. Same lowercase superscript letters in the same column indicate no significant differences ($P > 0.05$).

Table 3
Weibull analysis of the biaxial flexural strengths for two different 3D printed resins after thermocycling with different APA conditions. (SD: standard deviation, *m*: Weibull modulus, σ_o: characteristic strength, N: number of samples, R^2: Weibull distribution regression).

APA (μm, bar)	Materials (after thermocycling)	n	Flexural strength (MPa)		Weibull statistics		
			Mean	SD	*m*	σ_o	R^2
C	UDMA	14	134.57[a]	17.015	9.4291	141.71	0.9426
	BEMA	14	72.455[a]	17.343	5.0978	78.825	0.9064
501	UDMA	14	112.15[b]	12.550	10.483	117.61	0.8781
	BEMA	14	84.268[a]	15.098	6.2907	90.620	0.9371
502	UDMA	14	112.77[b]	20.665	6.1305	121.60	0.8231
	BEMA	14	71.277[a]	8.6475	9.8790	74.906	0.9342
503	UDMA	14	110.22[b]	14.391	9.1245	116.23	0.9518
	BEMA	14	74.170[a]	17.781	4.3394	81.844	0.8480
1101	UDMA	14	106.85[b]	13.735	8.9926	112.80	0.9042
	BEMA	14	71.036[a]	14.590	5.4549	77.013	0.9486
1102	UDMA	14	106.61[b]	10.615	12.069	111.13	0.9523
	BEMA	14	78.991[a]	16.714	5.5528	85.547	0.9023
1103	UDMA	14	108.29[b]	15.798	8.1141	114.83	0.9517
	BEMA	14	70.848[a]	10.823	7.4679	75.449	0.9679

C, control; UDMA, urethane dimethacrylate; BEMA, Bis-EMA. Same lowercase superscript letters in the same column indicate no significant differences ($P > 0.05$).

materials and elucidate the effect of thermocycling. At 50 MPa, all specimens demonstrated survival probabilities greater than 95 % before thermocycling. After thermocycling, all specimens, except BEMA503, had survival probabilities exceeding 90 %. At 75 MPa, the UDMA group maintained a survival probability above 99 % before thermocycling, whereas that of the BEMA group with 110 μm particles started to decrease below 90 %. After 75 days of thermocycling, the survival probability of the UDMA group remained over 90 %, whereas four of the seven BEMA group specimens exhibited survival probabilities below 50 %. Finally, the 100 MPa UDMA group maintained survival probabilities > 99 % before thermocycling and > 70 % after thermocycling. The survival probability of the BEMA group was above 70 % for the control test group and for the 50 μm APA group before thermocycling, and all of these specimens presented survival rates below 20 % after thermocycling. These specific comparisons of different specimens before and after thermocycling and with different APA treatments clearly highlight the decreased flexural strength values owing to thermocycling.

3.2. Nano-indentation

As presented in Fig. 4a, when the indentation strength increased from 2 N to 10 N for the UDMA sample, indentations of 21, 31.3, 38.3, 44.4, and 49.5 μm were recorded. When the pressing force was withdrawn, the indentation values were 12.1, 17.7, 21.5, 24.5, and 29.3 μm. By contrast, the indentation test results of the BEMA sample presented in Fig. 4b revealed indentation depths of 26.7, 38.4, 47.5, 54.2, and 58.3 μm. After the pressing force was withdrawn, the recovered values were 15.2, 22, 22, 27.5, 31.2, and 32.9 μm. When the UDMA and BEMA samples were tested under the same conditions, the UDMA resin presented a lower strain and higher recovery. The results of the 10 N experiment, which demonstrated the greatest difference, can be directly compared based on Fig. 4c.

3.3. DMA

Generally, when rheological properties are evaluated based on the dynamic mechanical testing of a material, the change in storage modulus related to the frequency should be confirmed. Supplementary Fig. S2a, which presents the analysis results for the UDMA sample, indicates that the storage modulus was 6828 MPa at 0.1 Hz and 7906 MPa at 68 Hz. Notably, the storage modulus increased with frequency. However, the BEMA composite analysis results presented in Supplementary Fig. S2b reveal that the storage modulus was 6058 MPa at 0.1 Hz and 9810 MPa at 100 Hz, which indicates a sharp increase compared to that in Supplementary Fig. S2a. The reason for this behavior is that the

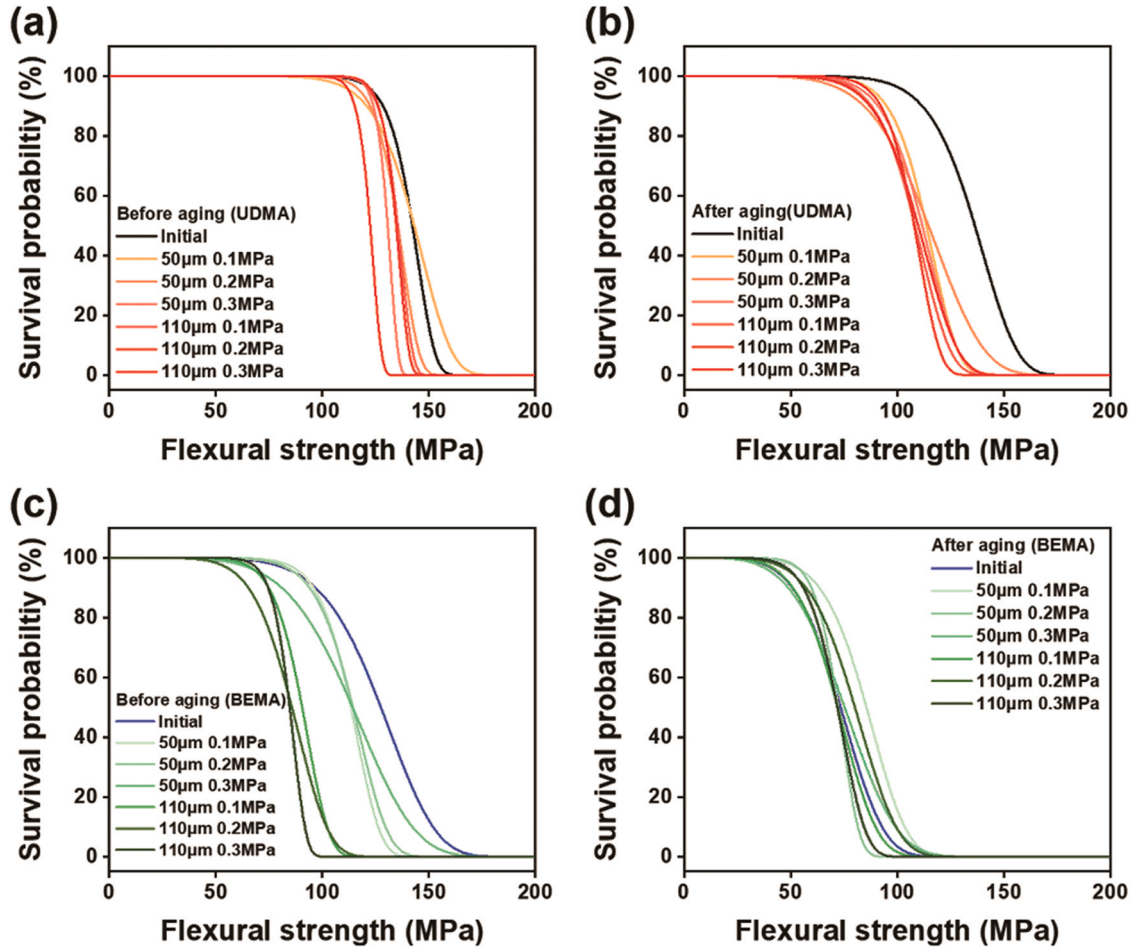

Fig. 3. Weibull survival probability based on the biaxial flexural strength (MPa) for two different materials sandblasted with particle sizes of 50 μm and 110 μm and pressures of 0.1, 0.2, and 0.3 MPa before and after thermocycling. (a) UDMA before thermocycling, (b) UDMA after thermocycling (c) BEMA before thermocycling, and (d) BEMA after thermocycling.

Table 4
Survival probability (reliability) of UDMA and BEMA resins before thermocycling at different APA conditions under compressive forces of 50 MPa, 75 MPa, and 100 MPa.

APA (μm, bar)	Materials (before thermocycling)	Survival probability (%)		
		50 MPa	75 MPa	100 MPa
C	UDMA	100	99.9995	99.8937
	BEMA	99.8836	99.161	87.6059
501	UDMA	99.9994	99.9470	98.7136
	BEMA	99.9925	99.3106	84.2575
502	UDMA	100	99.9998	99.7491
	BEMA	99.9747	98.7815	82.5058
503	UDMA	100	100	99.9951
	BEMA	99.2376	93.2446	71.4524
1101	UDMA	100	100	99.9733
	BEMA	99.7975	89.6271	15.6132
1102	UDMA	100	100	99.9892
	BEMA	98.3145	75.7924	13.4166
1103	UDMA	100	100	99.8659
	BEMA	99.9713	89.0284	0.0265

C, control; UDMA, urethane dimethacrylate; BEMA, Bis-EMA.

UDMA sample is composed of pure resin, whereas BEMA is a composite resin wherein inorganic hard particles are dispersed. Notably, inorganic particles dispersed within the BEMA resin resist material deformation and generate a higher storage modulus. At a frequency of 0.1 Hz, UDMA presents a higher storage modulus than BEMA. These results are consistent with the mechanical flexural strength test results obtained in this study. These results indicate that the strength of the polymer comprising the resin is higher for UDMA than that for BEMA. Additionally, because the storage/loss modulus transition does not occur when the test temperature of the sample is below the glass transition temperature (Tg), no unusual behavior is observed in the loss modulus and tan delta.

3.4. Roughness (R_a)

The effects of various alumina particle sizes and pressures on the surface roughness (R_a) of the specimens were investigated. The obtained R_a values are presented in Table 6, and the 3D surface morphology images of each group are presented in Figs. 5 and 6 and Supplementary Fig. S3. The R_a values in the UDMA group were significantly higher for the 0.3 MPa group with 50 μm particles and 0.2 MPa group with 110 μm particles than that in the control group. In the BEMA group, this value was significantly increased for the 0.3 MPa group with 50 μm particles and the 0.2 and 0.3 MPa groups with 110 μm particles compared to that for the control group.

3.5. SEM

Representative SEM images of each group are presented in Figs. 5 and 6 and Supplementary Fig. S3. Overall, smaller surface particles were observed in the BEMA group than in the UDMA group. The UDMA

Table 5
Survival probability (reliability) of UDMA and BEMA resins after thermocycling at different APA conditions under compressive forces of 50 MPa, 75 MPa, and 100 MPa.

APA (μm, bar)	Materials (after thermocycling)	Survival probability (%)		
		50 MPa	75 MPa	100 MPa
C	UDMA	99.9946	99.7523	96.3324
	BEMA	90.6450	46.0233	3.4615
501	UDMA	99.9872	99.1088	83.3048
	BEMA	97.6544	73.7721	15.5948
502	UDMA	99.5706	94.9636	73.974
	BEMA	98.1729	36.3333	2.9E-06
503	UDMA	99.9546	98.1808	77.6132
	BEMA	88.8837	50.4305	9.20454
1101	UDMA	99.9336	97.4844	71.2768
	BEMA	90.9581	42.0862	1.56552
1102	UDMA	99.9935	99.1353	75.6031
	BEMA	95.0576	61.7786	9.2610
1103	UDMA	99.8826	96.8956	72.2154
	BEMA	95.4751	38.4267	0.02754

C, control; UDMA, urethane dimethacrylate; BEMA, Bis-EMA.

group presented surface changes in contrast to the control group. Small particles and microcavities were observed in the UDMA501 group, whereas large particles and cavities were observed relatively uniformly in the UDMA503 group. Additionally, deep and wide cavities were observed in the UDMA1103 group. In the BEMA group, small particles were observed in the control group, whereas deep and thin cavities and cracks were observed in the surface-treated group. Sharp straight cavities were observed in the BEMA1102 and 1103 groups.

4. Discussion

This study evaluated the physical properties of materials used for APA surface treatments to determine the optimal surface treatment conditions for UDMA and BEMA materials. Because APA surface treatment is primarily used to improve the adhesion of restorations in the dental field, many studies of appropriate pressures and particle sizes have been reported. However, because no appropriate conditions for 3D printing materials as definitive restorations have yet been suggested, this study conducted experiments using various particle sizes and pressure conditions. Notably, the correlation between flexural strength and surface roughness according to the surface treatment is crucial. Thus, in this study, the roughness and flexural strength of the two types of 3D printing materials for final restorations were observed to significantly differ when the particles were large, and the surface was treated with APA under high pressure. A comprehensive analysis of flexural strength and surface morphology, including SEM and 3D imaging of the roughness, revealed that as the particle size and pressure of the printing material increased, deep defects and cracks formed on the surface, leading to the deterioration of physical properties. Consequently, the null hypothesis of this study was rejected.

APA has been recommended as a surface treatment to improve the bonding strength between currently used permanent restorations and teeth. In particular, several studies have reported that the APA treatment increases the mechanical strength of zirconia. Moreover, APA has been reported as an effective surface treatment method capable of generating a rough and clean surface and activating the surfaces of restorations. [29] However, for APA treatments, flaws on the surface, such as cracks in the resin matrix, can affect the flexural strength, which can be affected by APA conditions, that is, particle size or pressure [30,31]. Generally, the APA treatment uses hard particles to impact the

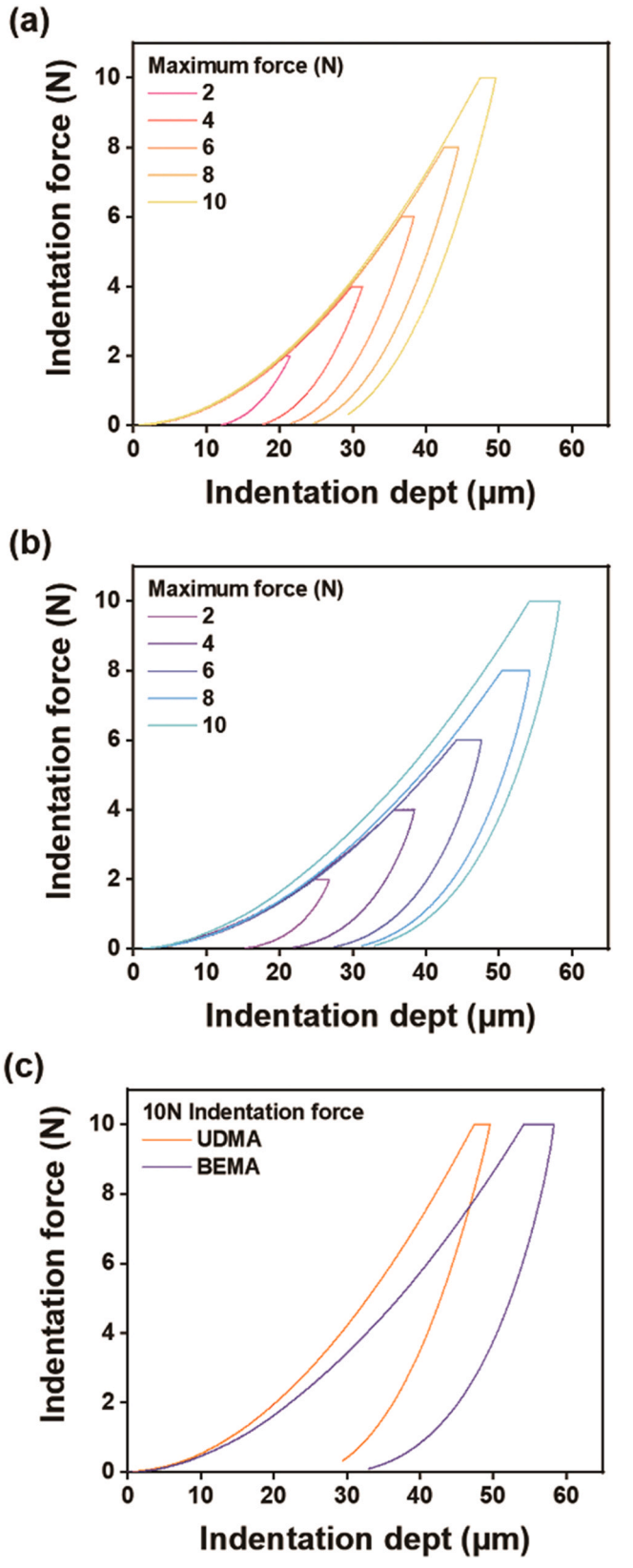

Fig. 4. Graph of the pressure-indentation characteristics of the nano-indentation experiment. (a) UDMA and (b) BEMA graph behavior of indentation deformation according to the maximum pressure from 2 to 10 N for BEMA resin. (c) Comparison between UDMA and BEMA at an indentation pressure of 10 N.

Table 6
Average surface roughness (R_a) values under each treatment condition.

	Surface average roughness ± SD (μm)						
	C	501	502	503	1101	1102	1103
UDMA	0.63 ± 0.05^{ab}	0.32 ± 0.04^{a}	0.93 ± 0.05^{b}	1.73 ± 0.16^{c}	0.62 ± 0.45^{ab}	1.62 ± 0.29^{c}	1.44 ± 0.20^{bc}
BEMA	0.68 ± 0.08^{a}	0.96 ± 0.68^{a}	1.29 ± 0.09^{ac}	2.34 ± 0.30^{bc}	1.10 ± 0.15^{ab}	2.77 ± 0.47^{c}	3.23 ± 0.74^{c}

SD, standard deviation; C, control; UDMA, urethane dimethacrylate; BEMA, Bis-EMA. Same lowercase superscript letters in the same row indicate no significant differences ($P > 0.05$).

target surface through pressure, which erodes the material and creates a rough surface to increase wettability. To the best of our knowledge, systematic experiments have been conducted to understand the effects of particle size and pressure on the surface changes and mechanical properties of various permanent materials under APA conditions. CAD/CAM restoration materials such as disperse-filled composites and polymer-infiltrated ceramic networks are polymers containing zirconia and ceramics requiring appropriate surface treatment, such as APA, for long-term mechanical maintenance. A particle size of 50 μm and pressure of 0.1–0.2 MPa are recommended as the conditions of APA to improve the adhesion of CAD-CAM materials [29,32]. A recent study on the adhesion between definitive restorative 3D printing resin and resin cement reported that applying APA to the surface of a 3D-printing resin effectively improved long-term bonding with cement [33]. However, reports on optimal pressure and particle size ranges within which only surface changes can be achieved without affecting the flexural strength of 3D printable permanent resin materials are absent. In this study, owing to APA treatment at different pressures using alumina particles of different sizes, we confirmed that the flexural strength of the two specimens decreased as the alumina particle size and air abrasion pressure increased. For the UDMA group, the flexural strength was lower in the UDMA1103 group compared to those of the control and UDMA501 groups; in the BEMA group, the flexural strength was lower in the 110 μm group compared to those of the control and 50 μm groups. These findings suggest the presence of an optimal APA condition that can change the surface of 3D printing resins without compromising the mechanical strength. Clinically, this could increase the adhesive strength without reducing the strength of the restoration, allowing for the selection and implementation of an APA condition for each material. However, further research is required to determine the optimal distance and time for APA application in a clinical setting.

A sound frequency sweep of the UDMA and BEMA resin samples used in this study revealed the properties of the composite material in the BEMA resin. UDMA was composed of pure resin and presented a low increase in the storage modulus despite an increase in the frequency; however, BEMA presented a lower storage modulus than UDMA at 0.1 Hz and a higher storage modulus than UDMA at 100 Hz. This behavior can be likely attributed to the fact that BEMA contains a large amount of inorganic fillers. Despite these differences, BEMA exhibited a greater strain and lower recovery than UDMA in the indentation test. These results indicate that the physical properties of the base polymer constituting the BEMA composite resin are inferior to those of the UDMA resin.

From the results of the DMA frequency sweep, it was found that the storage modulus of UDMA did not increase significantly even with an increase in the frequency, whereas in BEMA, the storage modulus increased by approximately 65% as the frequency increased. This can serve as an explanation for why UDMA presented a low decrease in physical properties after APA treatment and why the mechanical flexural strength significantly decreased in BEMA. Notably, BEMA exhibits increasingly brittle behavior with an increase in the instantaneous deformation. Furthermore, the larger the alumina particle size and the higher the pressure in the APA treatment process, the higher the instantaneous deformation, and the more brittle the material. By contrast,

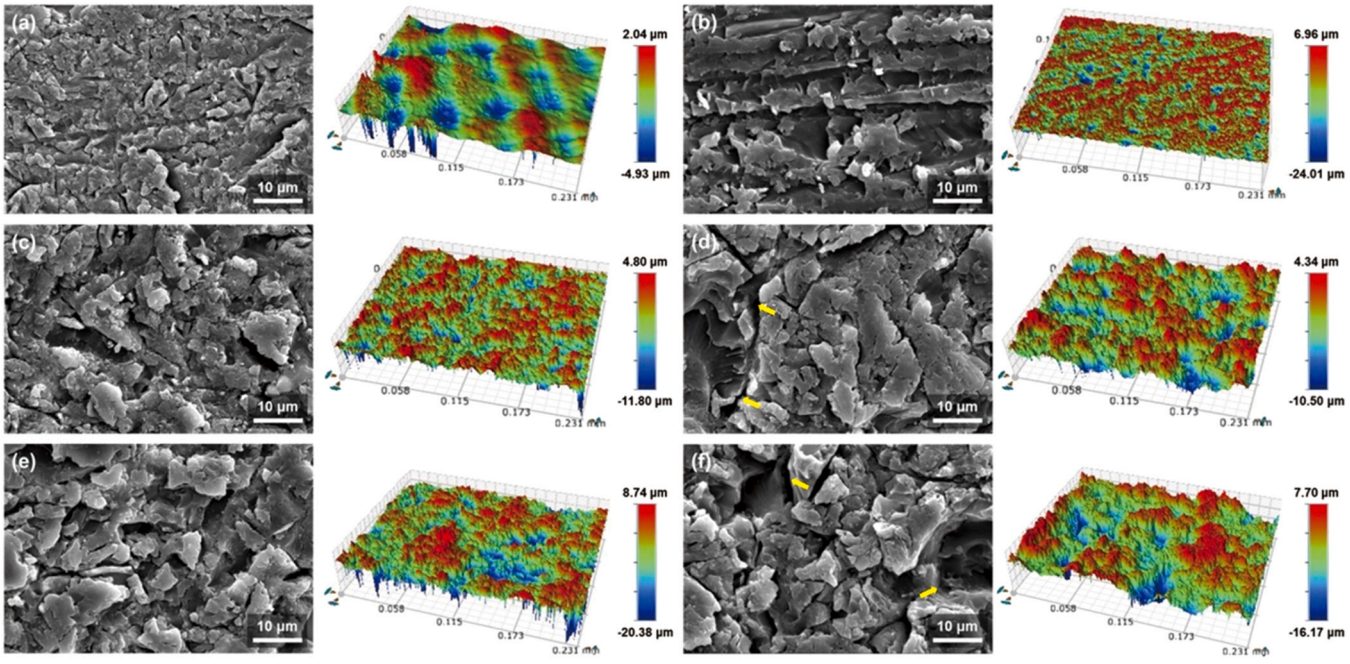

Fig. 5. Representative SEM images and 3D surface profiles of the surface images of UDMA according to various surface treatments: (a) UDMA, 50 μm, 0.1 MPa; (b) UDMA, 50 μm, 0.2 MPa; (c) UDMA, 50 μm, 0.3 MPa; (d) UDMA, 110 μm, 0.1 MPa; (e) UDMA, 110 μm, 0.2 MPa; and (f) UDMA, 110 μm, 0.3 MPa. Arrows indicate deep cavities and sharp cracks formation.

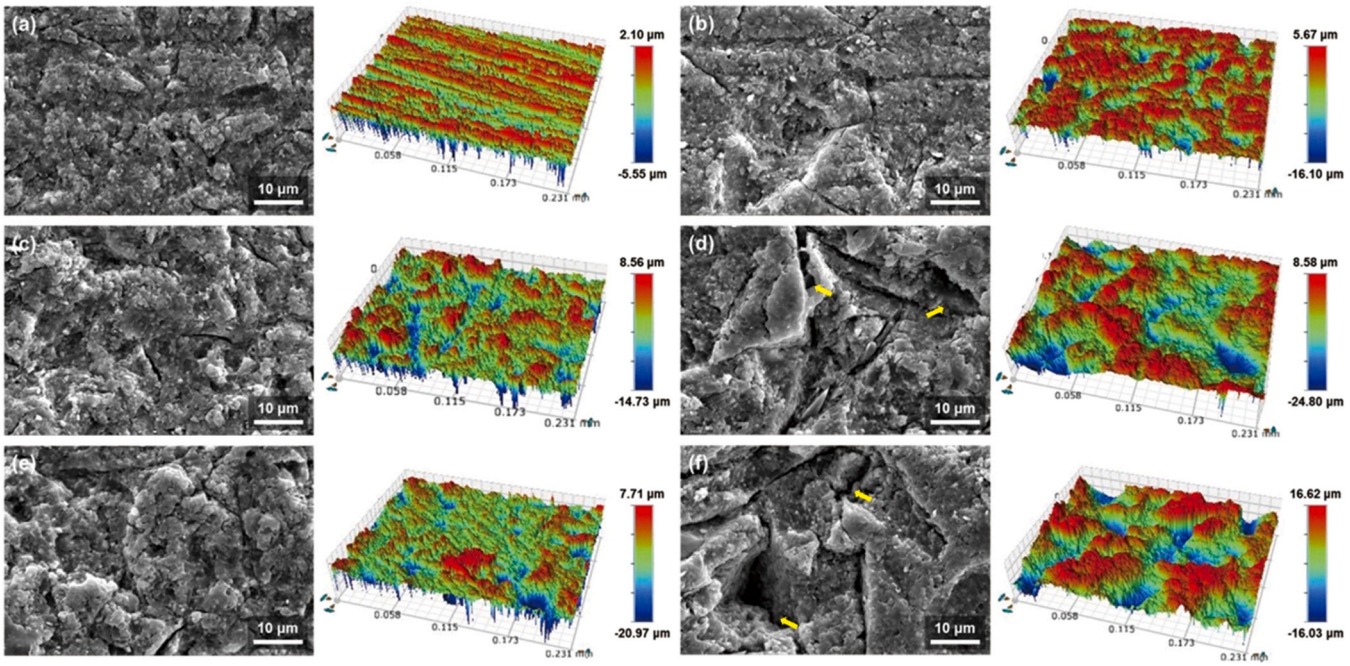

Fig. 6. Representative SEM images and 3D surface profiles of the surface images of BEMA according to various surface treatments: (a) BEMA, 50 μm, 0.1 MPa; (b) BEMA, 50 μm, 0.2 MPa; (c) BEMA, 50 μm, 0.3 MPa; (d) BEMA, 110 μm, 0.01 MPa; (e) BEMA, 110 μm, 0.2 MPa; and (f) BEMA, 110 μm, 0.3 MPa. Arrows indicate deep cavities and sharp cracks formation.

for UDMA, the storage modulus of the material was stable even when the instantaneous deformation was larger than that of BEMA. Therefore, the decrease in the mechanical flexural strength was not significant even after APA treatment.

In addition, based on the results of nano-indentation, it can infer that the maximum deformation and recovery of the UDMA and BEMA materials subjected to deformation under the same force were lower in the case of the UDMA materials. These results make it possible to infer the effect of alumina particles on the material surface during APA treatment. Combining the results of nano-indentation and DMA, it can conclude that UDMA has stable characteristics even when the amount of instantaneous deformation is large compared to that of BEMA, and it presents less deformation and high recovery under the same external force. Therefore, the decrease in mechanical flexural strength according to the APA treatment process is not large in UDMA; however, the decrease in BEMA is large.

The roughness was higher in the surface treatment groups than in the control group for both materials. In a previous study, when APA was performed at 0.2 MPa using 50 μm alumina particles on a PEEK surface, the R_a value was 0.9 μm, similar to that of UDMA502 in this study [34]. By contrast, the R_a value of the BEMA group was 1.29 μm under the same conditions, which was higher than that of the polymer material used in the previous study and that of the UDMA group. From the 3D surface morphology results, the UDMA group had a uniform surface owing to the generation of fine irregularities (Fig. 5). In the BEMA group, these surface irregularities were not uniform, and irregular deep parts were observed. Previous studies have reported that when a CAD/CAM block containing filler is treated with APA, the roughness and irregularity of the surface increase, and a structure capable of bonding with silane is formed while exposing the filler [32]. This is a similar result to that of our study. For the BEMA-containing filler, an irregular surface was formed as the filler was exposed. However, filler particles may be lost as cracks are generated on and below the surface of the resin matrix, which cannot increase the bonding strength owing to material damage [32]. UDMA is a resin that does not contain fillers; however, cracks may form on and below the surface of the material when treated with large particles and pressure. Therefore, in clinical practice, it is necessary to control the APA process according to the material to create a surface with proper adhesive strength without deteriorating strength in the long term.

As can be observed from the SEM images, the surface treatment of large-sized particles of aluminum oxide at high pressures induced the formation of microcracks, which decreased the flexural strength. When the surface treatment was performed at 0.2 MPa using small-sized aluminum particles, some untreated areas presented an unbalanced surface; however, there was no significant effect on the three-point flexural strength. When the two materials were compared, more cracks were observed in the BEMA than in the UDMA group. Thin and deep cavities and uneven surface changes could degrade material properties, and cracks would likely lead to fractures when a force is applied. In addition, when resin cement is used to adhere the materials to the teeth, the irregular surface and thin and deep cavities may lower the bonding strength with cement. In the case of the UDMA group, the surface is relatively uniform, and there are microcavities, which are expected to be advantageous for bonding with cement.

In this study, thermocycling was performed 10,000 times between 5 °C and 55 °C in water in 70 s cycles. As the long-term effectiveness of restorations is clinically essential, clinical safety was evaluated by reproducing long-term use. Generally, the thermocycling of a polymer involves two phenomena: thermal stress and water absorption. Water molecules penetrate the voids between the polymer chains and move further between the polymers, which expands the material [35]. These water molecules act as plasticizers promoting the movement of polymer chains and can cause a shape change as a plasticizing effect. This reaction is expected to cause a deterioration in the physical properties of the BEMA group. In the BEMA control group, it was estimated that the flexural strength decreased after thermocycling because of the water absorption and thermal stress occurring during the thermal cycle. By contrast, for the UDMA material, the oligomer constituting the material had low crystallinity and high molecular weight but was strongly bound

owing to the electronegativity of the monomer. With these characteristics, the appearance and disappearance of internal microcrystals do not occur during the thermal cycle; therefore, it is estimated that water absorption did not affect the UDMA group. In the UDMA group, after thermocycling, the flexural strength of all surface-treated groups decreased compared with that of the control group. However, no significant differences were observed between the surface-treated groups. This can be considered as a result of static fatigue in deep space due to thermal stress caused by a porous surface and subsurface exposure after the APA treatment, affecting the physical properties of the resin. However, because no difference was observed in the flexural strength between the surface treatment groups, it can be assumed that various surface treatment conditions did not affect long-term use.

Overall, this *in vitro* study suggests appropriate surface treatment conditions for permanent 3D printing resins with different components by studying the flexural strength according to the surface treatment of the two materials and the composition of each material. However, experiments evaluating the bonding strength according to surface treatment have not been conducted in this study. Because surface treatment is highly correlated with the shear bond strength of 3D printing resin, further studies should be conducted on the shear bond strength between a 3D printing resin for the final prosthesis and cement and its long-term aging effect.

5. Conclusions

The following conclusions can be drawn within the limitations of this *in vitro* study. The UDMA group exhibited a higher flexural strength and smaller decrease in this strength owing to surface treatments compared with the BEMA group. After thermocycling, the flexural strength decreased significantly in both the UDMA and BEMA groups. UDMA and BEMA presented porosity on the surface after the APA surface treatment. In particular, deep cracks and irregular deep areas were observed in the BEMA group treated with coarse particles under high-pressure conditions. To improve the adhesion and stability of the 3D printing resin for permanent restoration, it is necessary to consider surface treatment conditions that can increase the surface roughness without deteriorating physical properties according to each material component.

Acknowledgment

This study was supported by the Korea Medical Device Development Fund grant funded by the Korea government (the Ministry of Science and ICT, the Ministry of Trade, Industry and Energy, the Ministry of Health & Welfare, and the Ministry of Food and Drug Safety) (Project nos.: 1711174420, RS-2020-KD000260).

Appendix A. Supporting information

Supplementary data associated with this article can be found in the online version at doi:10.1016/j.dental.2023.05.007.

References

[1] Sulaiman TA. Materials in digital dentistry–a review. J Esthet Restor Dent 2020;32(2):171–81. https://doi.org/10.1111/jerd.12566
[2] Frazier WE. Metal additive manufacturing: a review. J Mater Eng Perform 2014;23(6):1917–28. https://doi.org/10.1007/s11665-014-0958-z
[3] Atzeni E, Salmi A. Economics of additive manufacturing for end-usable metal parts. J Adv Manuf Technol 2012;62(9):1147–55. https://doi.org/10.1007/s00170-011-3878-1
[4] van Noort R. The future of dental devices is digital. Dent Mater 2012;28(1):3–12. https://doi.org/10.1016/j.dental.2011.10.014
[5] Lee WS, Lee DH, Lee KB. Evaluation of internal fit of interim crown fabricated with CAD/CAM milling and 3D printing system. J Adv Prosthodont 2017;9(4):265–70. https://doi.org/10.4047/jap.2017.9.4.265
[6] Peng CC, Chung KH, Yau HT, Ramos V, Jr. Assessment of the internal fit and marginal integrity of interim crowns made by different manufacturing methods. J Prosthet Dent 2020;123(3):514–22. https://doi.org/10.1016/j.prosdent.2019.02.024
[7] Hwangbo NK, Nam NE, Choi JH, Kim JE. Effects of the washing time and washing solution on the biocompatibility and mechanical properties of 3D printed dental resin materials. Polymers 2021(24):13. https://doi.org/10.3390/polym13244410
[8] Jang W, Kook G-S, Kang J-H, Kim Y, Yun Y, Lee S-K, et al. Effect of washing condition on the fracture strength, and the degree of conversion of 3D printing resin. Appl Sci 2021;11:11676. https://doi.org/10.3390/app112411676
[9] Lim N-K, Shin S-Y. Bonding of conventional provisional resin to 3D printed resin: the role of surface treatments and type of repair resins. J Adv Prosthodont 2020;12(5):322–8. https://doi.org/10.4047/jap.2020.12.5.322
[10] Albahri R, Yoon H-I, Lee J, Yoon S, Lee S. Shear bond strength of provisional repair materials bonded to 3D printed resin. J Dent Sci 2020:16. https://doi.org/10.1016/j.jds.2020.05.003
[11] Park S-M, Park J-M, Kim S-K, Heo S-J, Koak J-Y. Flexural strength of 3D-printing resin materials for provisional fixed dental prostheses. Materials 2020;13(18):3970. https://doi.org/10.3390/ma13183970
[12] Bagheri A, Jin J. Photopolymerization in 3D printing. ACS Appl Polym Mater 2019;1(4):593–611. https://doi.org/10.1021/acsapm.8b00165
[13] Siripongpreda T, Hoven VP, Narupai B, Rodthongkum N. Emerging 3D printing based on polymers and nanomaterial additives: enhancement of properties and potential applications. Eur Polym J 2023;184:111806https://doi.org/10.1016/j.eurpolymj.2022.111806
[14] Zhang J, Xiao P. 3D printing of photopolymers. Polym Chem 2018;9(13):1530–40.
[15] Lin C-H, Lin Y-M, Lai Y-L, Lee S-Y. Mechanical properties, accuracy, and cytotoxicity of UV-polymerized 3D printing resins composed of Bis-EMA, UDMA, and TEGDMA. J Prosthet Dent 2020;123(2):349–54.
[16] Britto VT, Cantelli V, Collares FM, Bertol CD, Della Bona Á. Biomechanical properties of a 3D printing polymer for provisional restorations and artificial teeth. Dent Mater J 2022;38(12):1956–62.
[17] Nam NE, Shin SH, Lim JH, Shim JS, Kim JE. Effects of artificial tooth brushing and hydrothermal aging on the mechanical properties and color stability of dental 3D printed and CAD/CAM materials. Materials 2021(20):14. https://doi.org/10.3390/ma14206207
[18] Colombo M, Poggio C, Lasagna A, Chiesa M, Scribante A. Vickers micro-hardness of new restorative CAD/CAM dental materials: evaluation and comparison after exposure to acidic drink. Materials 2019(8):12. https://doi.org/10.3390/ma12081246
[19] Scribante A, Bollardi M, Chiesa M, Poggio C, Colombo M. Flexural properties and elastic modulus of different esthetic restorative materials: evaluation after exposure to acidic drink. BioMed Res Int 2019;2019:5109481. https://doi.org/10.1155/2019/5109481
[20] Grzebieluch W, Kowalewski P, Sopel M, Mikulewicz M. Influence of artificial aging on mechanical properties of six resin composite blocks for CAD/CAM application. Coatings 2022;12(6):837.
[21] Stawarczyk B, Basler T, Ender A, Roos M, Ozcan M, Hämmerle C. Effect of surface conditioning with airborne-particle abrasion on the tensile strength of polymeric CAD/CAM crowns luted with self-adhesive and conventional resin cements. J Prosthet Dent 2012;107(2):94–101. https://doi.org/10.1016/s0022-3913(12)60031-6
[22] Moon J-E, Kim S-H, Lee J-B, Han J-S, Yeo I-S, Ha S-R. Effects of APA protocol choice on the surface characteristics of monolithic zirconia materials and the shear bond strength of resin cement. Ceram Int 2016;42(1, Part B):1552–62. https://doi.org/10.1016/j.ceramint.2015.09.104
[23] Jeong KW, Kim SH. Influence of surface treatments and repair materials on the shear bond strength of CAD/CAM provisional restorations. J Adv Prosthodont 2019;11(2):95–104. https://doi.org/10.4047/jap.2019.11.2.95
[24] Lee K-S, Shin M-S, Lee J-Y, Ryu J-J, Shin S-W. Shear bond strength of composite resin to high performance polymer PEKK according to surface treatments and bonding materials. J Adv Prosthodont 2017;9(5):350–7.
[25] Murata H, Seo RS, Hamada T, Polyzois GL, Frangou MJ. Dynamic mechanical properties of hard, direct denture reline resins. J Prosthet Dent 2007;98(4):319–26. https://doi.org/10.1016/S0022-3913(07)60105-X
[26] Seong W-J, Kim U-K, Swift JQ, Hodges JS, Ko C-C. Correlations between physical properties of jawbone and dental implant initial stability. J Prosthet Dent 2009;101(5):306–18. https://doi.org/10.1016/S0022-3913(09)60062-7
[27] Abdalqadir M, Faraj S, Azhdar B. An evaluation of a technique to improve the mechanical properties of maxillofacial silicone elastomers with zinc oxide nanoparticles. J Prosthet Dent 2021. https://doi.org/10.1016/j.prosdent.2020.09.043
[28] Kim S-H, Choi Y-S, Kang K-H, Att W. Effects of thermal and mechanical cycling on the mechanical strength and surface properties of dental CAD-CAM restorative materials. J Prosthet Dent 2022;128(1):79–88. https://doi.org/10.1016/j.prosdent.2020.11.014
[29] Kim J-E, Lim J-H, Kang Y-J, Kim J-H, Shim J-S. Effect of pressure and particle size during aluminum oxide air abrasion on the flexural strength of disperse-filled composite and polymer-infiltrated ceramic network materials. Polymers 2020;12(6). https://doi.org/10.3390/polym12061396
[30] Marshall SJ, Bayne SC, Baier R, Tomsia AP, Marshall GW. A review of adhesion science. Dent Mater 2010;26(2):e11–6. https://doi.org/10.1016/j.dental.2009.11.157

[31] Yang B, Scharnberg M, Wolfart S, Quaas AC, Ludwig K, Adelung R, et al. Influence of contamination on bonding to zirconia ceramic. J Biomed Mater Res B Appl Biomater 2007;81(2):283–90. https://doi.org/10.1002/jbm.b.30664
[32] Yoshihara K, Nagaoka N, Maruo Y, Nishigawa G, Irie M, Yoshida Y, et al. Sandblasting may damage the surface of composite CAD-CAM blocks. Dent Mater 2017;33(3):e124–35. https://doi.org/10.1016/j.dental.2016.12.003
[33] Kang YJ, Park Y, Shin Y, Kim JH. Effect of adhesion conditions on the shear bond strength of 3D printing resins after thermocycling used for definitive prosthesis. Polymers 2023;15(6). https://doi.org/10.3390/polym15061390
[34] Lümkemann N, Strickstrock M, Eichberger M, Zylla I-M, Stawarczyk B. Impact of air-abrasion pressure and adhesive systems on bonding parameters for polyetheretherketone dental restorations. Int J Adhes 2017:80. https://doi.org/10.1016/j.ijadhadh.2017.10.002
[35] Takahashi Y, Hamanaka I, Shimizu H. Effect of thermal shock on mechanical properties of injection-molded thermoplastic denture base resins. Acta Odontol Scand 2012;70(4):297–302. https://doi.org/10.3109/00016357.2011.600719